e-palli

AMERICAN JOURNAL OF GEOSPATIAL TECHNOLOGY (AJGT)

ISSN: 2833-8006 (ONLINE)

VOLUME 3 ISSUE 1 (2024)

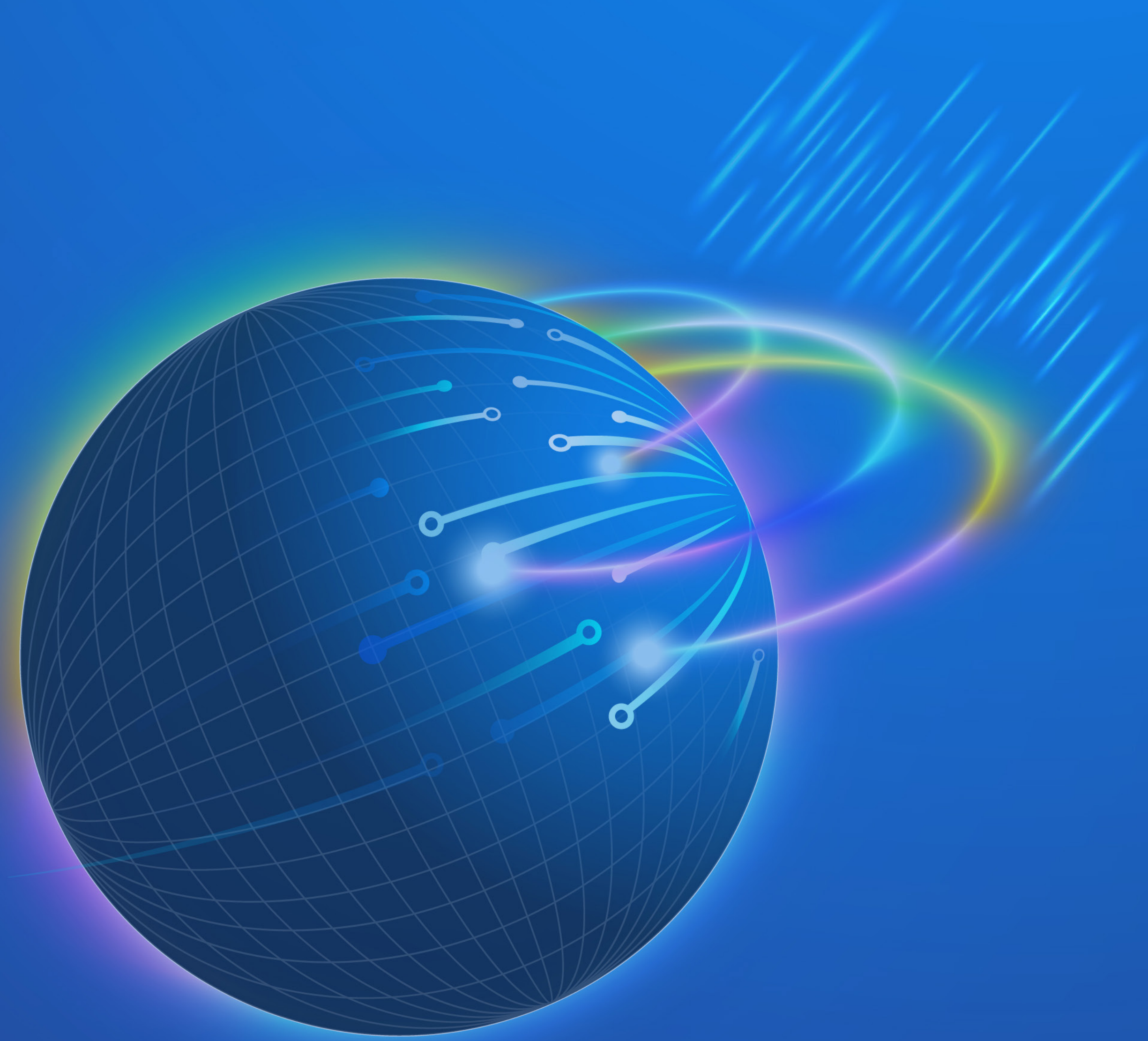

PUBLISHED BY
E-PALLI PUBLISHERS, DELAWARE, USA

American Journal of Geospatial Technology (AJGT)

Volume 3 Issue 1, Year 2024
ISSN: 2833-8006 (Online)
DOI: https://doi.org/10.54536/ajgt.v3i1.2882
https://journals.e-palli.com/home/index.php/ajgt

Steady-State Harmonic and Time Domain Point Absorber Modelling

Saad Al-Sahlawi[1*], Garvey Seamus[1], Kathy Johnson[1]

Article Information

Received: May 01, 2024

Accepted: May 27, 2024

Published: June 01, 2024

Keywords

Heaving Point Absorber, Damping, Steady-State Harmonic Model, Time Domain Model, Power Take-Off (PTO), Buoy Shape Optimisation, Resonance

ABSTRACT

This paper analysed the development of a steady-state harmonic model which, along the vertical axis, can simulate a single buoy's motion with one degree of freedom (heave). The model can optimise a buoy's geometric and control parameters to maximise power absorption from incident waves. The steady-state model revealed that at resonance, maximum power absorption of the buoy occurred in two region values with either low or high range of values of radiation damping coefficient (c2). In practice, achieving operation in the low c2 region is difficult. Therefore, it is recommended that the devices be designed to operate in the high c2 region to increase power capture. The model also revealed the best value for c1 (PTO damping coefficient) when the buoy with the peak frequency of the sea state is at resonance, and its mass is optimum. The PTO device size can therefore be manufactured accordingly to maximise power absorption. Out of all the tested buoy shapes (spike, bullet, and bi-cone), the bi-cone (60°/120°) buoy performed the best, and its response was most similar to the optimum mass response predicted by the model.

INTRODUCTION

Increasing the energy absorption of heaving point absorbers under regular waves is focused on tuning the Wave Energy Conversion (WEC) system to oscillate in resonance with the incoming waves (Al Shami *et al.*, 2018; Pastor & Liu, 2014). If a point absorber buoy is in resonance with incident waves, it will see increased displacement amplitudes and velocities and absorb more energy than when it is not (Falnes & Kurniawan, 2020; Kara, 2020). To achieve the resonance, the phase and amplitude of the point absorber oscillation have to be chosen carefully to ensure optimal performance. Phase and amplitude can be varied independently through phase and amplitude control factors (Cruz, 2007; Sinha *et al.*, 2016). When maximum power absorption is achieved, these control factors are considered optimal for a desired point absorber motion. This can be calculated for a single buoy in multiple degrees of freedom motion or a single degree of freedom motion (Ahmed *et al.*, 2022). An optimal result can be obtained by forcing the amplitude and phase to take particular values (Haider *et al.*, 2021). The various stages required to convert the power absorbed from a wave to the final useful energy are as follows:

- Stage One is the flow of power between wave (0) and primary interface (1), which gives the intercepted power.
- Stage Two is the power flow between the primary interface and the (PTO) (2), giving the captured power.
- Stage Three is the power flow between the PTO and the final power conversion stage (3), giving the delivered power.

In a point absorber system, the buoy is connected to a PTO-driven generator to capture the wave-induced motion and turn it into electrical power. A point absorber is a mechanical system with two parameter sets, including control and geometrical parameters (Bubbar & Buckham, 2020). The structure of the buoy is defined by geometrical parameters, which are unchanged once the buoy is built (Sun *et al.*, 2021). The control parameters are related to the PTO damping mechanism, also known as variable parameters that can be tuned to match a given sea state. The focal point of the WEC devices is motion control, which aims to increase the performance and competitiveness of particular devices in the energy market. Therefore, numerous techniques are used, including latching and unclutching or phase control (Salter *et al.*, 2002; Tona *et al.*, 2019). They have been developed and applied to wave devices to improve efficiency and minimise energy production costs. These will be discussed in detail below.

With regular waves, the maximum power absorption for a heaving point absorber WEC can be achieved when:

1. The excitation force of the waves is in phase with the velocity profile of the device (Rahmati & Aggidis, 2016).
2. The velocity excursion of the wave cycle maximized when energy is supplied (Rahmati & Aggidis, 2016).

The second condition requires very complex PTO mechanisms; it is rarely considered. However, a few types of solutions have been proposed for condition one. These include:

Linear Damping

Applying a constant linear damping coefficient (Nolan *et al.*, 2005).

Freewheeling or Declutching

By allowing the device to freewheel (unloaded) from the extrema (i.e., causing velocity to increase and later applying

[1] Department of Mechanical Engineering, University of Nottingham, Nottingham NG7 2RD, United Kingdom
[*] Corresponding author's e-mail: SaadAl-Sahlawi@outlook.com

load only after a specific threshold of velocity is reached) (Garcia-Rosa & Ringwood, 2015; Salter *et al.*, 2002).

Latching

Locking the buoy at the instant in a position when its velocity reaches zero and releasing it after a specific period (Budar & Falnes, 1975; Saupe *et al.*, 2014).

LITERATURE REVIEW

Early theoretical works showed that a single-point absorber could capture power from a wave crest width greater than the width of the buoy itself, giving potential greater power extraction when collecting power from a given length of the beach. The heave amplitudes required for maximum power extraction are available only in resonant conditions for real buoys. Outside resonant frequencies, the power absorbed decreases markedly (Kara, 2016). Additionally, the power absorption of a semi-submerged sphere was plotted as a function of wave frequency. At resonant frequencies with no frictional damping, a linear PTO damper (generator) 's power recovery reached the theoretical maximum (Kurniawan *et al.*, 2014). However, on either side of the resonant frequency, the dynamic heaving response of the buoy was insufficient to reach the levels required for maximum theoretical power recovery (Duncan & Brown, 1982). Another study reviewed the physical aspects related to this behaviour. It noted that to broaden a buoy's frequency response, the external PTO damping coefficient should be set higher than the optimum at resonance (Sakr *et al.*, 2020).

Studies have also been undertaken to optimise the hydrodynamic performance of various WEC devices to improve their energy extraction efficiency from waves. Nonetheless, PTO damping, buoy geometry, and supplementary inertia are significant for phase control (Aderinto & Li, 2019). They maximise efficiency and increase the capture width of a heaving point absorber device deployed in the North Sea off Belgian coastlines (Piscopo *et al.*, 2016). A point absorber's performance was assessed in multiple studies where the resonance was tuned by changing the PTO characteristics. Results depicted an increased power capture in the regular waves by 50% of the rated power (Al Shami *et al.*, 2018). In addition, a past study examined irregular waves, analyzing that maxmised power capture can be achieved by continuously tuning the natural frequency to the incoming wave frequency (Burgaç & Yavuz, 2020). Falcao (2007) performed a time domain analysis to examine the hydrodynamic performance of a coupled hydraulic PTO unit and heaving floating device. An algorithm was developed for the performance optimisation of the device, showing performance on the wave period to be dependent weakly irrespective of wave height simulated in conditions of the real sea (Falcão, 2007). He further examined and included a phase control strategy of latching in the frequency domain to increase power absorption (Falcão, 2008). In his next paper, a two-body heaving point absorber's geometrical configuration was optimised using phase control in the frequency domain (Falcao, 2010).

Al Shami *et al.* reviewed multiple studies analysing the effects of geometry, mass distribution, and mooring system on a tethered WEC in irregular waves. Results revealed that tuning the system for a specific wave climate is critical for avoiding potential WEC failure and maximum energy capture (Al Shami *et al.*, 2018). Reportedly, Sjokvist *et al.* (2014) utilised a velocity ratio to study the impact of radius and buoy draft on WEC energy and motion absorption. Findings showed that an optimal buoy geometry can be identified for a given generator damping. When designing the point absorber, the velocity ratio was more informative than the capture width ratio. For example, the optimum buoy radius for 7.4 kNs/m, 20 kNs/m, and 30 kNs/m of damping is around 1.75 m, 2.5 m, and 3 m, respectively. For damping of 20 kNs/m and 30 kNs/m, however, there was no difference in the results for buoy radius values of 2.5 m, 3 m, or 3.5 m. While larger buoys were more favourable with increasing damping, smaller buoys were favourable with lower damping (Sjökvist *et al.*, 2014). Another study showed the modeling of a PTO system, demonstrating that oversimplification during the simulation phase of WEC development can lead to incorrect design decisions and additional delays and costs (Cargo *et al.*, 2016).

Using phase control to shift the natural frequency of a point absorber near the resonance condition by adding a supplementary mass or a negative mechanical spring has also been studied (Piscopo *et al.*, 2016). They also showed that phase control tunes the natural frequency of the device suitably into the fully submerged body based on PTO damping. Passive control was also studied by Piscopo *et al.* (2016), combined with the development of a new optimisation process for heaving point absorber hydrodynamic performance to maximize energy production yearly. Their optimisation procedure allows for modifying the PTO damping and fully submerged added mass until the optimum configuration is detected. It was concluded that the deployment site is essential in the WEC assessment for optimum configuration (Piscopo *et al.*, 2016).

A new approach for optimising the geometry and performance of a point absorber was proposed in this paper, to increase wave device efficiency while minimising energy production costs. A steady-state harmonic model was designed to simulate motion with one degree of freedom (heave) along the vertical axis of a single buoy. It is used to optimise its geometrical and control parameters, and its power absorption is maximised from incident waves. The steady-state harmonic model was verified against a time domain model by comparing the models' predictions for steady state response. The geometrical and control parameters of the heaving buoy were optimised to achieve a cost-effective buoy design that maximised power absorption from incident waves. The buoy behaviour was simulated for the case of regular waves. The approach used was numerical, and the dynamic equations were formulated, and the results were calculated in the time domain using the software MATLAB. The PTO damper c_1 was assumed to be a constant damping coefficient for simplicity, and the force of force was decomposed into a linear radiation-damping term c_2 which reflected the system geometry. Further analyses were carried out to determine the damping profiles of varied buoy shapes: bullet, spike, and bi-cone ($60^o/120^o$).

Generalised Heaving Point Absorber (Buoy) Model Point Absorber System

The basic design and functional principles of a point absorber system are illustrated in Figure 2, which shows a rigid floating body (buoy) attached to the sea bed. The purpose of the floating buoy is to act as the energy-absorbing body of the system and hold the system upright. These two functions result from the buoyancy of the buoy and the induced pressure forces due to water particle movement in the wavefront. The generator consists of a spring-damper system where the PTO provides the damping. The generator's primary function is to take the energy captured from the wave-induced motion of the float by the PTO and convert it into electricity. The PTO device is placed somewhere between the sea bed and the buoy to determine the direction of the buoy's motion, which is crucial for power production. The generator also contains a spring, which acts as a pre-tensioner to keep the line straight. The point absorber buoy system, which has a mass, a damping coefficient, and a stiffness coefficient in classical mechanics, can be treated as a mass-spring-damper system.

The buoy system is modelled as rigidly attached to the generator to move the entire system in phase. This is one of the main assumptions used in the analysis presented in this paper.

When the point absorber buoy system is displaced

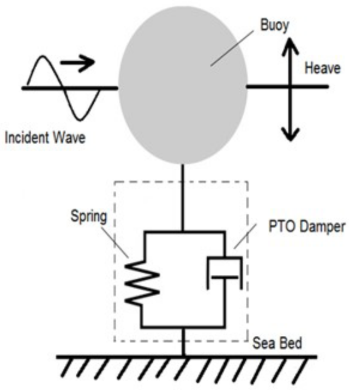

Figure 1: Basic design of a point absorber system

from equilibrium, a restoring force proportional to its displacement is experienced. Notably, the system is called a simple harmonic oscillator if the only force acting on the system is the restoring force (Korde & Ringwood, 2016). This means that, with a constant amplitude and frequency, it undergoes simple harmonic motion. If the force is proportional to the velocity, the damped oscillator is the harmonic oscillator (Fitzpatrick, 2018). Using the damping coefficient, the system can:

- Oscillate with a frequency lower than in the non-damped case, and the displacement amplitude decreases with time (underdamped system).
- Decay to the equilibrium position without any oscillation (overdamped system).

The boundary between overdamped and underdamped behaviour occurs at a specific value of damping coefficient where the system is called "critically damped." In this case, the damping coefficient is called the critical damping coefficient, c_c, is given by:

$$c_c=2\sqrt{km}\ \text{(Ns/m)} \tag{1}$$

The ratio of the actual damping coefficient to the critical damping coefficient is called the damping ratio,ξ, and is given by:

$$\xi=c/c_c \tag{2}$$

Mass-Spring-Damper Representation

In this model, a point absorber system's simple motion is compared to a mechanical oscillator containing a mass-spring-damper system with a single degree of freedom of motion working in the direction of the degree of freedom subjected to an external force. Figure 3 presents a schematic representation of the system.

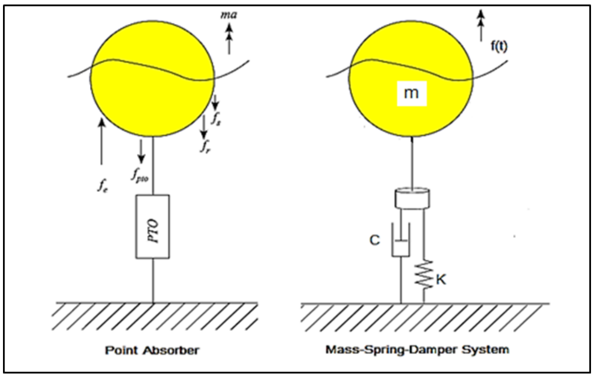

Figure 2: Schematic representation of mass-spring-damper system

The system's damping is linear with a damping coefficient, c (Ns/m). A harmonic force is applied with angular frequency, ω (rad/s) and amplitude, A (m). The spring constant, k (N/m) to the system, is a restoring mechanical force proportional to the system's vertical displacement, y, from its original position.

Time Domain Model

The Equation of motion of this buoy can thus be found from Newton's second law:

$$m\ddot{y}+(c_1+c_2)\dot{y}+ky=A\ [k\cos(\omega t)-c_2\ \omega\sin(\omega t)] \tag{3}$$

Equation (3) was linearised by expressing each term on the left-hand side as a velocity function. The buoy relative velocity v(t) was then calculated using the Runge-Kutta 4th order method in MATLAB (suitable for non-stiff cases) by setting.(y) (t)= $\dot{v}(t)$ and $\dot{y}(t)=v(t)$ and applying the initial conditions $\dot{y}(0)= v(0) = 0$. Based on the results, the rate of energy dissipation in the damper over time t_1 was computed and is given as:

$$E_d (t_1)=\int_0^{t1} P_1 \, dt= \int_0^{t1} c_1 \, \dot{y}^{2\, dt} \quad (4)$$

In theory, this energy is maximised when Equation (4) is maximised over one period of the excitation wave force. It results in the condition:

$$\omega_n = c_1 \sqrt{(k/m)}= \omega \quad (5)$$

When this condition is met, the device's velocity profile is in phase with the excitation wave force, consistent with condition one for maximising the power absorption.

Equation of Motion

Due to the vertical wave velocity u(t), the buoy is displaced from its equilibrium position to an actual position of y(t). The differential Equation of motion of the point absorber can be found in Newton's second law:

$$m\ddot{y}+ c_1 \dot{y} = k (u-y)+ c_2 \; (\dot{u}- \dot{y}) \quad (6)$$

The spring force is expressed in Equation (6) as k (u-y). The damping force exerted by the PTO system is expressed as $c_1 \dot{y}$. The damper c_1 is the main power extraction unit, and the PTO system is assumed to be linear for simplicity. The radiation force is expressed as $c_2 \; (\dot{u}- \dot{y})$.

Power Absorption

The velocity,v, in the power extraction damper c_1 is expressed as:

$$v(t)=(y(t)) = Re\,(V\times e^{j\omega t}) \quad (7)$$

The mean power extracted by damper c_1 is given by:

$$P= 1/2 \, c_1 \, |j\omega Y|^2 = 1/2 \; c_1 \, \omega^2 \; |Y|^2 \quad (8)$$

Substituting Equation (7) into Equation (8) gives:

$$P= 1/2 \, \omega^2 \, c_1 \times ((k^2 + \omega^2 c_2^2))/(((k- \omega^2 m)^2+ \omega^2 \; (c_1+ c_2)^2)) \times U^2 \quad (9)$$

It can be seen that although the wave magnitude,U, does not affect the optimal values of m, c_1 and c_2, it can affect the value of the extracted power.

Power Absorption Optimisation

To optimise the buoy power extraction rate, the term H defined below needs to be differentiated concerning m, c_1 and c_2. The partial derivatives $\partial H/\partial m$, $\partial H/(\partial c_1)$ and $\partial H/(\partial c_2)$ are then set equal to zero, and their stationary values are obtained.

$$H= (c_1 \, (k^2 + \omega^2 c_2^2))/(((k- \omega^2 m)^2+ \omega^2 \, (c_1+ c_2)^2)) \quad (10)$$

Setting the numerator in the partial derivative $(\partial H/\partial m)$ equal to zero gives the stationary values for m as:

$$m= k/\omega^2 \quad (11)$$

Setting the numerator in the partial derivative $(\partial H/(\partial c_1))$ equal to zero, substituting for $m= k/\omega^2$ and rearranging gives:

$$c_1 = c_2 \quad (12)$$

Setting the numerator in the partial derivative $(\partial H/(\partial c_2))$ equal to zero, and rearranging gives:

$$c_2 = k^2/(\omega^2 \, c_1) \quad (13)$$

By substituting for m from Equation (11) and c_2 from Equation (13) into Equation (9), the expression for the optimum power extraction rate was obtained as follows:

$$P= 1/2 \times (\omega^2 \, c_1 \, k^2)/((\omega^2 \, c_1^2 + k^2)) \times U^2 \quad (14)$$

The system has 5 dimensions: k,m,c_1,c_2 and ω. To reduce the number of dimensions when calculating the buoy optimum power response, m was fixed at its optimum value and c_1 was fixed at its reference value. The unknown parameter c_2 was varied for a wave magnitude U = 1 m. The buoyancy-stiffness and wave natural frequency were kept constant at k =10006 N/m and $\omega=2\pi$ rad/s. The natural frequency of the buoy was assumed to be equal to the peak frequency of the sea state, i.e., it was assumed to be in resonance. Optimisation of the buoy power response was carried out in MATLAB using the following:

PTO external damping coefficient $c_1= k/\omega$ (Ns/m).

Buoy mass $m= k/\omega^2$ (kg).

Radiation damping coefficient $c_2 = c_c \, [10^{(-8)}$ to $10^8]$ (Ns/m). The c_2 value was varied using 500 time steps.

RESULTS

The first set of simulations was performed by fixing m and c_1 at their optimum values and varying c_2 to determine the optimum power extraction rate over the range of regular wave conditions. The mean power extracted was determined using Equation (9), and the results are plotted in Figure 3.

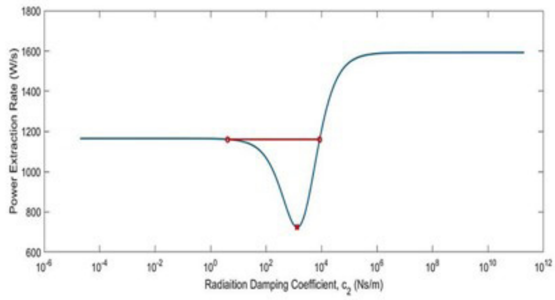

(a) Buoy mass = 100 kg

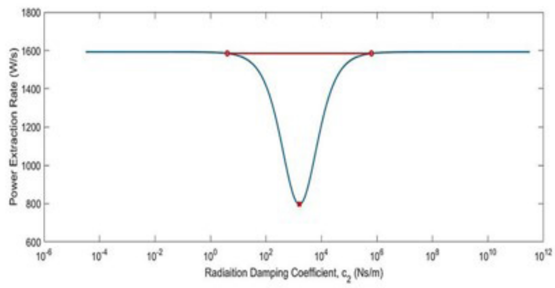

(b) Buoy mass = 253.4549 kg

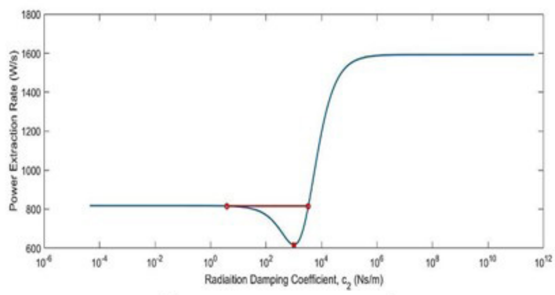

(c) Buoy mass = 500 kg

Figure 3: Power capture at c_1= 1592.50 Ns/m and m= (a) 100 kg (b) 253.4549 kg, and (c) 500 kg

The results indicate that there are two power extraction rate regions: the left region is driven by the low value of c_2 and the right region is driven by the high value of c_2 as seen in Figure 3. With this model, the optimum mass and value of c_1 were found to be 253.4549 kg and 1592.50 Ns/m, respectively (Figure 3b).

It was clear from the simulations that using the optimum mass gave the highest power extraction rates in the right and left regions of the graph (Figure 3a). The power extraction rate was constant for $c_2<10^2$ and $c_2>10^4$ (Ns/m), and the lowest power extraction rates occurred for c_2 values between 10^2 and 10^4 (Ns/m). These results are similar to the results from the time domain model.

Further analyses were conducted with mass values above and below the optimum mass. Mass values of 100 kg (Figure 3a) and 500 kg (Figure 3c) resulted in only lower power capture in the left region. This showed that there is no visible effect of increasing the mass to 500 kg when the c_2 value is high. Mass was only found to play a significant role in low values of c_2. The maximum power extraction rate of a buoy with optimum mass $\tilde{m}$ and $\tilde{c}_1$ was 1585 W/s.

Validation

The time for time domain and steady-state harmonic models to reach steady state was 60s, and the maximum power absorption achieved for both models was 36.53 kW. The results from both analyses were almost identical. This indicated that the steady-state harmonic model developed for analysing the steady-state conditions of the WEC system gave good predictions for buoy behaviour. Therefore, the steady-state harmonic model was utilised for further optimisation.

Steady-State Harmonic Model

In this section, the steady-state model is presented, and oscillation of a point absorber in a harmonic wave is discussed to a fixed reference. The buoy is restricted to heave motion only. It is assumed that one end of the system is fixed to an inertial frame similar to the time domain model discussed in the previous section. A schematic of a point absorber system under vertical wave velocity u(t) is shown in Figure 4.

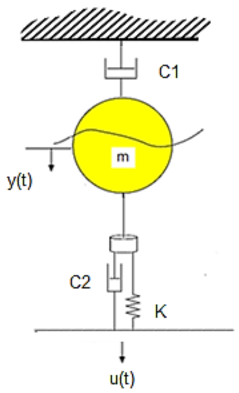

Figure 4: Schematic representation of a heaving point absorber

Steady-State Harmonic Model Optimisation

The objective of this section is to examine the optimal damping profile for a point absorber (buoy) using the values for c_1 and c_2 which gave the greatest power absorption. The shape is assumed to be independent of the specific device parameters for the optimal damping profile.

From Equation (12), the optimum performance is achieved when $c_1 = c_2$. The power response was thus maximised by using the best value for c_2 from the region driven by high c_2 for determining the best value of c_1 for a mass equal to the optimum mass.

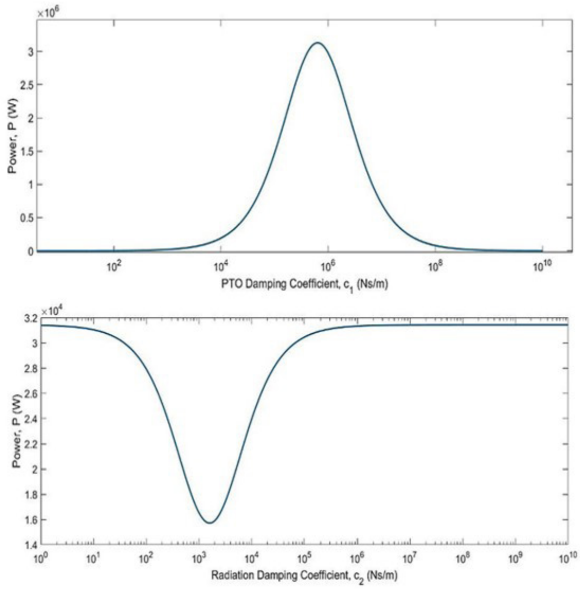

Figure 5: Power capture at $c_1 = 6.54 \times 10^5$ Ns/m and $c_2 = 6.54 \times 10^5$ Ns/m

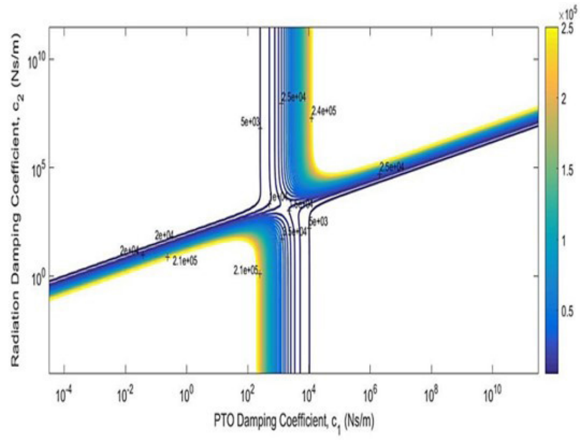

Figure 6: Contour plot for the relationship between c_1 and c_2 at $\tilde{m}$

RESULTS

For the resonance condition, the best value of the PTO damping coefficient c_1 for the optimal radiation damping coefficient $c_2 = 6.54 \times 10^5$ Ns/m is illustrated in Figure 5. The results of the simulation confirm the validity of the linear relationship derived in Equation (12) (see the contour plot of $c_1 = c_2$ in Figure 6).

From Figure 7, it can be seen that the highest power occurs at $c_1 = c_2$ with the optimum mass of 253.4549 kg. The value of c_2 is defined by the structure of the buoy and cannot be changed once the buoy has been constructed. The term c_1 is used to model the PTO damping mechanism, a variable parameter that can be tuned to match the sea state. It is therefore recommended that buoys are constructed with large c_2 values such that the optimum c_1 value will equal c_2 and will not change when the system is not at resonance.

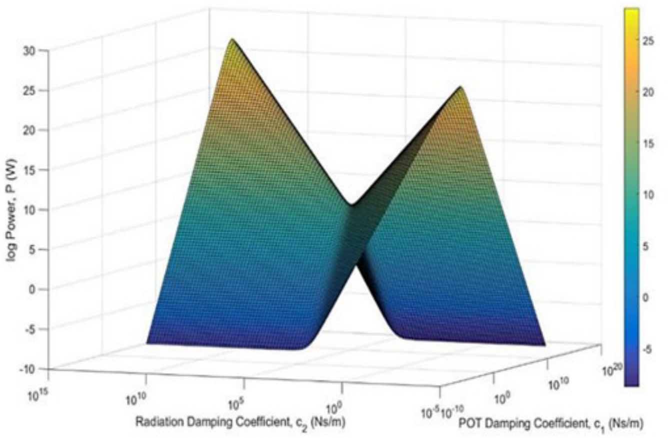

Figure 7: Log power vs c_1 and c_2 at $\tilde{m}$ = 253.4549 Kg

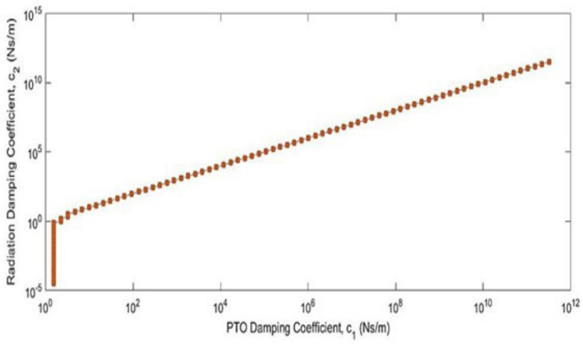

(a) mass equals 99.99 % of $\tilde{m}$

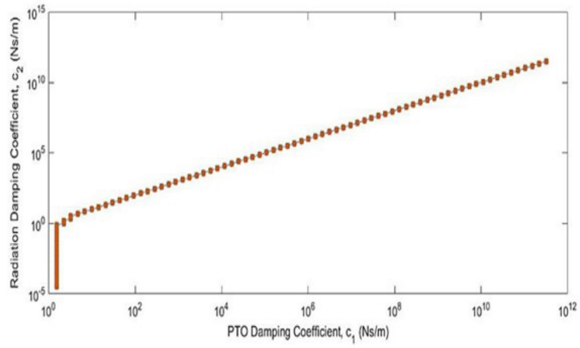

(b) optimum mass $\tilde{m}$

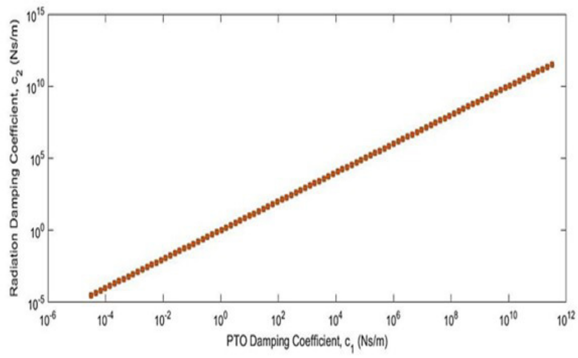

(c) mass equals 100.01 % of $\tilde{m}$

Figure 8: The relationship between c_1 and c_2 with m

At optimum mass, the system is in resonance, and to maximise the power absorbed, the condition of $c_1 = c_2$ must be met. Further analyses were conducted with mass values of 99.99% and 100.01% of $\tilde{m}$. The tests revealed that for a system that is not in resonance, the linear relationship between c_1 and c_2 no longer holds. This was true even when mass deviated by only 0.01% from its optimum value, as seen in Figures 8a and 8c.

It was concluded that the relationship $c_1 = c_2$ is only valid if the point absorber is at its optimum mass (Figure 8b) and is in resonance with the peak frequency of the sea state.

Buoy Shape Optimisation

Validating the steady-state harmonic model against experimental data was conducted. The steady-state harmonic model determined the optimal damping profiles for different point absorber (buoy) shapes. As already shown, wave energy extraction is a complicated procedure, and every change in the geometrical or control parameters has a major impact on the system's power extraction. It was therefore decided to carry out the optimisation process by keeping the diameter of the buoys fixed and comparing the buoys purely based on their shape and draft.

The damping characteristics of the three different point absorber (buoy) shapes were determined experimentally, and the results were compared against those of the steady-state harmonic model to determine the optimum operating region for each buoy shape. Three buoy shapes were chosen, namely (a) bullet, (b) spike, and (c) bi-cone ($60^o/120^o$). The dimensions of the buoy prototypes are illustrated in Figure 9.

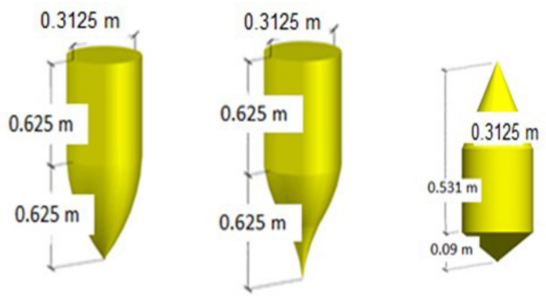

Figure 9: Shapes and dimensions of prototype buoys

All the shapes have the same cross-sectional area (diameter = 0.3125 m) but have different mass and draft values, as shown in Table 1 in the next section. The bullet and spike buoys had relatively longer drafts (0.755 m) than the bi-cone buoy (0.22 m).

Table 1: Bullet, spike, and bi-cone decay tests and statistical results

Buoy Shape	Mean Damping Ratio	Buoy Mass (kg)	Mean Draft (m)	Mean Damped Frequency (Hz)	Mean Radiation Damping Coefficient, C_2 (Ns/m)	Sample Variance s^2 $(Ns/m)^2$
Spike	0.128	27.72	0.755	0.729	32.51	3.6074
Bullet	0.124	33.44	0.755	0.667	34.84	9.2916
Bi-cone	0.094	11.63	0.220	1.164	16.0	7.8795
Damped Spike	0.114	27.30	0.755	0.727	28.51	0.8511
Damped Bullet	0.111	31.24	0.755	0.685	29.54	10.5423
Extra Damped Spike	0.099	27.58	0.755	0.715	24.55	5.3399
Extra Damped Bullet	0.095	31.01	0.755	0.693	25.55	2.37

Decay tests were performed at the Kuwait Institute for Scientific Research (KISR) utilising the Coastal Management Program's wave flume tank facility. The approach for this work consisted of two parts: (a) conducting decay tests to determine the radiation-damping coefficient, c_2, for each buoy shape; and (b) examining the behaviour of each buoy under different damping conditions. Only the bullet and spike buoys were used for part (b). The different damping conditions were achieved by adding one (damped) or two (extra-damped) round disks to the lower section of the buoys. When two disks were used, they were attached 2 cm and 3 cm apart for the bullet and spike buoys, respectively. After testing, the values of c_2 obtained from the decay tests were verified by checking whether they were close to the worst c_2 value obtained from the optimised steady-state harmonic model or approached the best c_2 values.

Buoy Power Optimisation

To optimise the power absorbed by each buoy at resonance and under zero damped, damped, and extra damped conditions, the steady-state harmonic model was used to determine the optimal. c_2 damping profiles for each shape. The values of c_2 obtained during decay testing were verified to ensure they were not near the worst c_2 value obtained from the model. All the damping coefficient values were scaled down to match the physical models. The diameter used for the steady-state harmonic analyses was d = 1 m, and the physical models had d = 0.3125 m.

The performance of the bullet, spike, and bi-cone buoys was optimised using the following hydrodynamic parameters in MATLAB:

Buoyancy-stiffness corresponding to an occupied area of 0.08 m2 in seawater, $k = (\pi d^2/4) \times 9.81 \times 1000$ N/m.

Wave frequency, $\omega = 2\pi = 6.28$ rad/s.

Resonance frequency, $\omega_n = 2\pi/0.9$ rad/s. This was calculated based on the experimental results, which gave resonance at T= 0.9 s (see Chapter 4).

Mass = mass of buoys used in the decay tests (see Table 3.1).

Radiation damping coefficient c_2=damping ratio × c_c (Ns/m). The damping ratio of each buoy shape was taken from the decay tests and used to determine c_2 the value associated with it.

Radiation damping coefficient $c_2 = c_c$ $[(10^{-8})$ to $(10^8)]$ (Ns/m). The c_2 value in the model was varied using 500-time steps.

RESULTS

During the experimental testing, the opportunity to vary the performance of the buoys at very little cost was utilised. Based on the steady-state harmonic model predictions, it was concluded that operating in the high-damping region is recommended to maximise the power extraction rate, which suggests that adding some form of damping is beneficial. This was tested during the experimental investigation, and extra damping was provided in the form of round discs mounted on the lower parts of the bullet and spike buoys. A comparison between the mean c_2 values for all the shapes were collected; the results are illustrated in Figure 10.

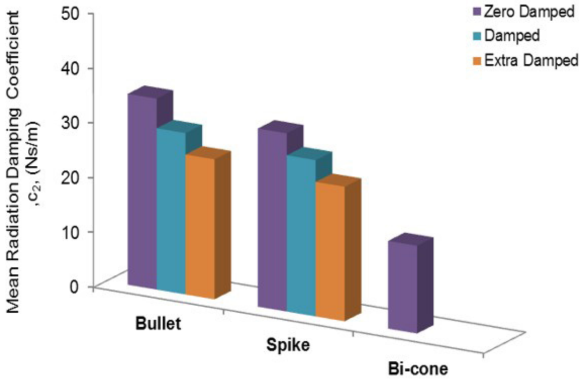

Figure 10: Mean c_2 for the bullet, spike, and bi-cone buoys

The extra-damped bullet and spike buoys had the lowest radiation-damping values compared to the zero-damped and damped buoys. This behaviour was confirmed by the statistical t-test, where probabilities above 95% provided very high confidence in the results.

The variation in the power absorbed by the zero-damped buoys as a function of the radiation-damping values is illustrated in Figures 11a, 11b, and 11c. In these figures, the c_2 values derived from the decay tests for each shape are marked in blue and the worst c_2 values from the model are marked in red.

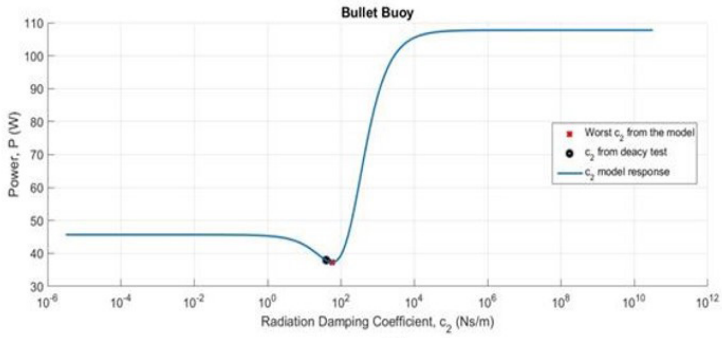

(a) Bullet buoy

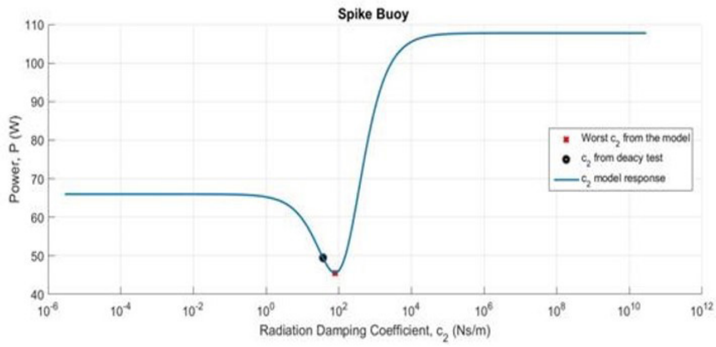

(b) Spike buoy

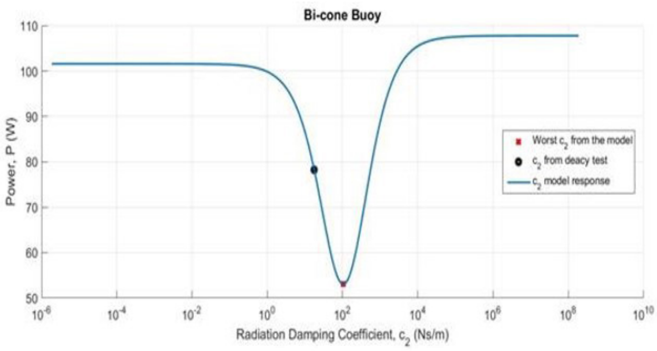

(a) Bi-cone buoy

Figure 11: Maximum power capture at $\tilde{c}_2$ for zero damped buoys

Figures 11a and 11b, for the bullet and spike buoys, respectively, showed lower power capture in the left-low c_2 region only. This means that their mass is far from optimum, as indicated in Figure 3, which shows results for masses above and below optimum. The c_2 values for the bullet and spike buoy shapes are close to the worst values for c_2 predicted by the model. In Figure 11a, for the bullet buoy, the power recorded in the highest and lowest c_2 regions were 107.78 W and 45.67 W, respectively. The worst power region for the bullet buoy occurred for c_2 between 2.41 and 1.51 × 104 Ns/m. For this buoy to achieve a power absorption of 107.78 W, its c_2 the value should be higher than 1.51 × 104 Ns/m.

CONCLUSION

A new approach for optimising the geometry and performance of a point absorber was proposed to increase wave device efficiency while minimizing energy production costs. The simulation of the motion of a single buoy for a steady-state harmonic oscillator model was attempted with one degree of freedom (heave) to optimise control and geometric parameters along the vertical axis. It is vital for maximisation of the power absorption from incident waves. The steady-state harmonic model was verified against a time domain model by comparing the models' predictions for steady-state response. The geometrical and control parameters of the heaving buoy were optimised to achieve a cost-effective buoy design which maximised power absorption from incident waves. The buoy behaviour was simulated for the case of regular waves. The approach used was numerical, and the dynamic equations were formulated, and the results were calculated in the time domain using the software MATLAB. The PTO damper c_1 was assumed to be a constant damping coefficient for simplicity, and the radiation force was decomposed into a linear radiation-damping term c_2 which reflected the system geometry. Further analyses were carried out to determine the damping profiles of different buoy shapes: bullet, spike, and bi-cone (60°/120°).

The steady-state model revealed that at resonance, maximum power absorption of the buoy occurred in two region values with either low or high range of values of radiation damping coefficient. In practice, it is critical to achieve operation in the low c_2 region; therefore, it is advised to use the devices designed with high c_2 region to maximise power capture. This suggests that external damping should be added to the buoy structure. The results also indicated that there was an optimum operating range for each buoy shape for the PTO-driven generator where wave energy capture is greatest and thus the electrical power. The model revealed that the best value for c_1 is $c_1= c_2=k/\omega$, when the buoy is in resonance with the peak frequency of the sea state and its mass, is optimum. The PTO device size can therefore be manufactured accordingly to maximise power absorption. Out of all the tested buoy shapes (spike, bullet, and bi-cone), the bi-cone (60°/120°) buoy's response was most similar to the optimum mass response predicted by the model, which indicated that its mass of 11.63 kg was closest to optimum. It was also noted that the c_2 damping associated with the tested bi-cone shape was quite different from the c_2 value predicted by the model to give the worst performance. The optimisation approach developed could be used to realise major economic design benefits for any point absorber buoy shape. The model presented in this work provides an analytical framework for an improved understanding of point absorber PTO devices.

Future Developments

The PTO system has been modelled as a linear damper. This might be considered the models' main limitation because approaches that consider irregular waves tend to be more accurate as they better replicate real sea conditions. In reality, the linear approach is invalid, and power losses due to the PTO will always be present. The PTO system thus needs to be modelled more accurately.

An extensive study on modelling a PTO system can be conducted where existing literature could be used further to improve the steady-state harmonic model in this work. Cargo (2012) demonstrated that over-simplification of the PTO during the phase of simulation of WEC development could lead to subsequent delays and costs and incorrect design decisions. Therefore, future studies need to consider economic considerations during the design process. The radiation damping drives optimal design parameters such as buoy shape, dimensions, and structure c_2 which in turn is dependent on the costs involved.

Nomenclature

A Amplitude of excitation force [m]
A_w Area occupied by the buoy in seawater [m^2]
c Damping coefficient [Ns/m]
c_1 PTO damping coefficient [Ns/m]
$\tilde{c}_1$ Optimum PTO damping coefficient [Ns/m]
c_2 Radiation damping coefficient [Ns/m]
$\tilde{c}_2$ Optimum radiation damping coefficient [Ns/m]
c_a Actual damping coefficient [Ns/m]
c_c Critical damping coefficient [Ns/m]
K Spring constant, used to represent buoyancy-stiffness [N/m]
M Mass [kg]
$\tilde{m}$ Optimum mass [kg]
P Power absorbed by the PTO [W]
S Standard deviation in results
T Time [s]
u(t) Wave vertical velocity [m/s]
V Velocity across damper [m/s]
x(t) Wave displacement [m]
Y Vertical displacement [m]
$\dot{y}$ & v Vertical velocity [m/s]
$\ddot{y}$& $\dot{v}$ Vertical acceleration [m/s2]
ξ Damping ratio
λ Frequency of displacement for calculating time constant

Ø Amplitude of displacement for calculating time constant
τ Time constant representing time to settle to steady state
η Overall power absorption efficiency [%]
ω_α Angular frequency of excitation force [rad/s]

Acknowledgements
The authors wish to express their gratitude and thanks for the University of Nottingham and Kuwait Scientific Research Centre (KISR) for providing all the infrastructure facilities to carry out this work.

REFERENCES

Aderinto, T., & Li, H. (2019). Review on power performance and efficiency of wave energy converters. *Energies, 12*(22), 4329.

Ahmed, A., Wang, Y., Azam, A., & Zhang, Z. (2022). Design and analysis of the bulbous-bottomed oscillating resonant buoys for an optimal point absorber wave energy converter. *Ocean Engineering, 263,* 112443.

Al Shami, E., Zhang, R., & Wang, X. (2018). Point absorber wave energy harvesters: A review of recent developments. *Energies, 12*(1), 47.

Bubbar, K., & Buckham, B. (2020). On establishing generalized analytical phase control conditions in two body self-reacting point absorber wave energy converters. *Ocean Engineering, 197,* 106879.

Budar, K., & Falnes, J. (1975). A resonant point absorber of ocean-wave power. *Nature, 256*(5517), 478-479.

Burgaç, A., & Yavuz, H. (2020). Power capture performance of a heaving wave energy converter for varying b rad/b pto ratio. *SN Applied Sciences, 2*(10), 1679.

Cargo, C., Hillis, A., & Plummer, A. (2016). Strategies for active tuning of Wave Energy Converter hydraulic power take-off mechanisms. *Renewable Energy, 94,* 32-47.

Cruz, J. (2007). Ocean wave energy: current status and future prespectives. Springer Science & Business Media.

Duncan, J. H., & Brown, C. E. (1982). Development of a numerical method for the calculation of power absorption by arrays of similar arbitrarily shaped bodies in a seaway. *Journal of Ship Research, 26*(01), 38-44.

Falcao, A. F. d. O. (2010). Wave energy utilization: A review of the technologies. *Renewable and sustainable energy reviews, 14*(3), 899-918.

Falcão, A. F. d. O. (2007). Modelling and control of oscillating-body wave energy converters with hydraulic power take-off and gas accumulator. *Ocean Engineering, 34*(14-15), 2021-2032.

Falcão, A. F. d. O. (2008). Phase control through load control of oscillating-body wave energy converters with hydraulic PTO system. *Ocean Engineering, 35*(3-4), 358-366.

Falnes, J., & Kurniawan, A. (2020). Ocean waves and oscillating systems: linear interactions including wave-energy extraction (Vol. 8). Cambridge university press.

Fitzpatrick, R. (2018). Oscillations and waves: an introduction. CRC Press.

Garcia-Rosa, P. B., & Ringwood, J. V. (2015). On the sensitivity of optimal wave energy device geometry to the energy maximizing control system. *IEEE Transactions on Sustainable Energy, 7*(1), 419-426.

Kara, F. (2016). Point absorber wave energy converters in regular and irregular waves with time domain analysis. *International Journal of Marine Science and Ocean Technology, 3*(7), 74-85.

Kara, F. (2020). A Control strategy to improve the efficiency of point absorber wave energy converters in complex sea environments. *Journal of Marine Science Research and Oceanography, 3*(2), 46-54.

Korde, U. A., & Ringwood, J. (2016). Hydrodynamic control of wave energy devices. Cambridge University Press.

Kurniawan, A., Greaves, D., & Chaplin, J. (2014). Wave energy devices with compressible volumes. *Proceedings of the Royal Society A: Mathematical, Physical and Engineering Sciences, 470*(2172), 20140559.

Nolan, G., Ringwood, J., Butler, S., & Leithead, W. (2005). Optimal damping profiles for a heaving buoy wave energy converter. ISOPE International Ocean and Polar Engineering Conference,

Pastor, J., & Liu, Y. (2014). Frequency and time domain modeling and power output for a heaving point absorber wave energy converter. *International Journal of Energy and Environmental Engineering, 5,* 1-13.

Piscopo, V., Benassai, G., Cozzolino, L., Della Morte, R., & Scamardella, A. (2016). A new optimization procedure of heaving point absorber hydrodynamic performances. *Ocean Engineering, 116,* 242-259.

Rahmati, M., & Aggidis, G. (2016). Numerical and experimental analysis of the power output of a point absorber wave energy converter in irregular waves. *Ocean Engineering, 111,* 483-492.

Sakr, A. H., Metwalli, S. M., & Anis, Y. H. (2020). Dynamics of heaving buoy wave energy converters with a stiffness reactive controller. *Energies, 14*(1), 44.

Salter, S. H., Taylor, J., & Caldwell, N. (2002). Power conversion mechanisms for wave energy. Proceedings of the Institution of Mechanical Engineers, *Part M: Journal of Engineering for the Maritime Environment, 216*(1), 1-27.

Saupe, F., Gilloteaux, J.-C., Bozonnet, P., Creff, Y., & Tona, P. (2014). Latching control strategies for a heaving buoy wave energy generator in a random sea. *IFAC Proceedings Volumes, 47*(3), 7710-7716.

Sinha, A., Karmakar, D., & Soares, C. G. (2016). Performance of optimally tuned arrays of heaving point absorbers. *Renewable energy, 92,* 517-531.

Sjökvist, L., Krishna, R., Rahm, M., Castellucci, V., Hagnestål, A., & Leijon, M. (2014). On the optimization of point absorber buoys. *Journal of marine science and engineering, 2*(2), 477-492.

Sun, P., Hu, S., He, H., Zheng, S., Chen, H., Yang, S., & Ji,

Z. (2021). Structural optimization on the oscillating-array-buoys for energy-capturing enhancement of a novel floating wave energy converter system. *Energy conversion and management, 228,* 113693.

Tona, P., Sabiron, G., & Nguyen, H.-N. (2019). An energy-maximising MPC solution to the WEC control competition. International Conference on Offshore Mechanics and Arctic Engineering.